Propagation Over Clutter: Physical Stochastic Model

Dmitry Chizhik and Jonathan Ling

***Abstract*—Propagation of radio signals from a base above clutter, such as buildings and trees, to a mobile immersed in clutter is treated theoretically by accounting for random diffuse scattering at the mobile. Small-scale fading and distance-dependent loss are treated in a unified way, as opposed to the heuristic methodologies, which formulate them as separate factors. Closed form expressions are derived for path gain and for angular spectrum at the base in both urban and heavily foliated environments. The resulting predictions are in close agreement with widely accepted models and empirical results. The angular spectrum at the base in urban environments is found to be Lorentzian of width close to that reported for measurements in Aarhus. In foliated environments, vegetation is represented as statistically homogeneous diffuse scattering medium, resulting in a Gaussian-shaped angular spectrum at the base.**

***Index Terms*—Angle spread, radio propagation.**

I. Introduction

PERFORMANCE of wireless communication systems is ultimately limited by the channel characteristics. While propagation loss is important in determining received signal strength for all wireless links, angular spread is needed to describe the small-scale fading behavior, such as fading dynamics, diversity, and spatial multiplexing performance of multiantenna wireless channels. In this paper, channel characteristics of macro-cellular systems are considered, characterized by a base station placed above large-scale clutter, such as buildings and trees and a mobile station that is close to the ground and immersed in clutter. Behavior of such channels is often described heuristically as a combination of several observed effects [1]. The received signal strength is represented as a product of three factors, path loss whose value in decibels depends linearly on the logarithm of transmitter-receiver separation, a "shadow-fading" factor, which is modeled statistically as a log-normally distributed random variable, and a small-scale fading factor, often described as being Rayleigh distributed. Empirical models of the distance dependent path loss that have gained widespread acceptance include the Hata model [2] based on Okumura's data [3] and its modifications [4], as well as the Erceg–Greenstein model [5], both based on finding a linear fit to measured path loss data. Analytical models of path loss include the Walfisch–Bertoni model [6] that describes propagation over buildings as a sequence of diffractions over half-space screens, followed by a final diffraction at the last roof-edge towards the mobile. Whitteker [7] represented propagation over clutter using physical-optics techniques, followed by a single diffraction towards the mobile. Blaunstein [10] represents propagation loss as a consequence of probabilistic visibility representation and interaction with multiple random scatterers. The small-scale fading characteristics are usually not considered in such analytical treatments, presumably to be added as a separate factor. Separate measurement studies have been carried out reporting the power angular spectrum at the base station in urban environments, e.g., [13]. In this paper, propagation modeling is carried out by explicitly considering random diffuse scattering at street-level in the vicinity of the mobile and propagation over clutter as a deterministic problem. This is an extension of the work in [9] that now properly accounts for the small-scale effects of random scattering at the mobile allowing modeling of path loss. Resulting simple closed-form expressions for path loss as well as for power angular spectrum at the base are found to be in good agreement with previously reported results.

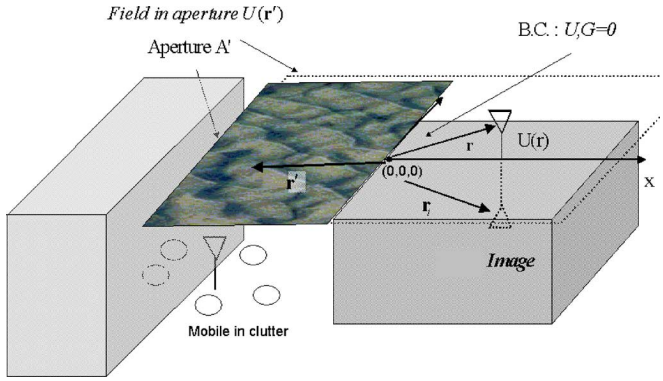

Fig. 1. Canonical outdoor environment. The wave-like pattern over the street aperture is the interference pattern of the field that results from multiple scattering in the vicinity of the mobile.

II. Problem Formulation

Terrain covered by large-scale clutter, such as houses and trees, is represented by a dielectric slab, shown in Fig. 1. The signal radiated by the mobile antenna produces a field U. The scalar field U represents the horizontal H field in the case of vertical polarization and the horizontal E field in the case of horizontal polarization. This scalar field representation is strictly valid only where there is no cross-polarization coupling, which is not considered here. The radiated signal is scattered from the local objects (e.g., building walls, trees, cars, etc.) in the vicinity of the mobile, represented by circles around the mobile in Fig. 1.

Above the large scale clutter the environment is taken as a homogeneous medium (i.e., air, neglecting ionospheric scatter) in which the field U satisfies the scalar Helmholtz equation

$$\nabla^2 U + k^2 U = 0 \tag{1}$$

Manuscript received July 13, 2006; revised June 4, 2007.

The authors are with Bell Laboratories, Alcatel-Lucent, Holmdel, NJ 08904 USA (e-mail: chizhik@alcatel-lucent.com).

Color versions of one or more of the figures in this paper are available online at http://ieeexplore.ieee.org.

Digital Object Identifier 10.1109/TAP.2008.919163

where $k = 2\pi/\lambda$ is the wavenumber. The field radiated by the mobile and measured at the base station may be expressed in terms of the values of the field and its gradient at a boundary, chosen here to be the horizontal plane just above the dielectric slab, by using the Helmholtz–Kirchhoff theorem

$$U(\mathbf{r}) = \iint d\mathbf{A}' \cdot \left(U(\mathbf{r}') \nabla G(\mathbf{r}, \mathbf{r}') - G(\mathbf{r}, \mathbf{r}') \nabla U(\mathbf{r}') \right). \tag{2}$$

The Green's function $G(\mathbf{r}, \mathbf{r}')$ represents the field at location $\mathbf{r}$ due to a point source at $\mathbf{r}'$. It is the point source response of the environment and serves a role similar to the impulse response in linear system theory, while (2) may be thought of as a superposition integral. In the case of a flat surface, representing flat terrain with uniform height clutter, the integration in (2) is over the horizontal plane boundary $z' = 0$ and $G(\mathbf{r}, \mathbf{r}')$ may be derived using the image method as

$$G(\mathbf{r}, \mathbf{r}') = \frac{e^{ik|\mathbf{r}'-\mathbf{r}|}}{4\pi|\mathbf{r}'-\mathbf{r}|} + R_s \frac{e^{ik|\mathbf{r}'-\mathbf{r}_i|}}{4\pi|\mathbf{r}'-\mathbf{r}_i|} \tag{3}$$

where $\mathbf{r}' = (x', y', z')$ points to the integration boundary, and $\mathbf{r} = (x, y, z)$ and $\mathbf{r}_i = (x, y, -z)$ point to the base station antenna and its image, respectively. The origin is defined in Fig. 1 to be at the roof edge near the mobile. In (3) R_s is the specular reflection coefficient of the surface representing top of the clutter illuminating the area above the mobile antenna at a grazing angle $\theta = \tan^{-1} z/x$, where z is the base antenna height above clutter and x is the horizontal separation (range) between the mobile and the base. For $z \ll x$, the grazing angle is very small, and the reflection coefficient $R_s \approx -1$ for dielectric surfaces over a wide range of permittivity values, [14], [15], for both parallel (here vertical) and perpendicular (here horizontal) polarization, leading to fields satisfying the Dirichlet boundary condition, $U(x, y, 0) = 0$. This is in contrast to perfectly conducting surfaces where the reflection coefficient for parallel polarization is $+1$ and the Neumann boundary condition applies, $\partial U(x, y, z)/\partial z|_{z=0} = 0$. Notably, measurements of received signal strength in rural Line-of-Sight conditions using vertically polarized antennas reported received signal power decaying with range x as $1/x^4$, consistent with the Dirichlet boundary conditions. At large ranges Neumann boundary condition would result in $1/x^2$ decay of received signal power, at odds with both theory and observation. The requirement that the clutter surface be perfectly flat may be somewhat relaxed, provided that the root mean square (rms) surface roughness σ satisfies the Rayleigh criterion, $4\pi\sigma \sin\theta/\lambda \ll 1$ [15]. Setting $R_s = -1$ in (3)

$$G(\mathbf{r}, \mathbf{r}') = \frac{e^{ik|\mathbf{r}'-\mathbf{r}|}}{4\pi|\mathbf{r}'-\mathbf{r}|} - \frac{e^{ik|\mathbf{r}'-\mathbf{r}_i|}}{4\pi|\mathbf{r}'-\mathbf{r}_i|}. \tag{4}$$

The Greens function $G(\mathbf{r}, \mathbf{r}')$ (4) is thus zero over the entire boundary. This allows the second term in the integrand of (2) to drop out, leading to

$$U(\mathbf{r}) \approx \int_{-\infty}^{\infty} dy' \int_{-\infty}^{\infty} dx' U(x', y', 0) \left.\frac{\partial G}{\partial z'}\right|_{z'=0}. \tag{5}$$

Using the Fresnel approximation for the distance R between the base antenna (or its image) and the street aperture

$$\begin{aligned} R &= \sqrt{(x-x')^2 + (y-y')^2 + (z-z')^2} \\ &\approx (x-x') + \frac{x'^2 + (y-y')^2 + (z-z')^2}{2x} \end{aligned} \tag{6}$$

for range x much larger than antenna separation or the size of the street aperture, $x \gg x', y', z', y, z$, the vertical derivative of the Greens function in (5) may be written as

$$\left.\frac{\partial G}{\partial z'}\right|_{z'=0} = \left.\frac{\partial G_e}{\partial z'}\right|_{z'=0} \exp\left(ikx' + \frac{ik(y-y')^2 + ikx'^2}{2x} \right) \tag{7}$$

where G_e is the Greens function evaluated above the edge of the street aperture $(0, 0, z')$ near the mobile

$$G_e = G(x, 0, z|0, 0, z'). \tag{8}$$

The exponential factor in (7) continues the Green's function from the aperture edge at $x' = 0$, $y' = 0$, $z' = 0$ to other points in the plane $z' = 0$ using the Fresnel approximation (6).

The field $U(x', y', 0)$ is the result of multiple scattering of the field radiated by the mobile from objects in the street and walls of the surrounding buildings. Such scattering is usually associated with small scale fading. Analysis of extensive measurements of azimuth and elevation angular spectra for macrocellular scenario [17] reported wide spread in both azimuth and elevation, attributed to multiple scattering around the mobile, as opposed to single roof edge diffraction. In other words, the signal emitted by the mobile antenna is multiply scattered from objects in the street containing the mobile, some of which may eventually strike the roof edge at a large range of angles and be diffracted towards the base. As the locations and geometries of scattering objects are not presumed to be known, it is of interest to find two statistical quantities: the spatial correlation of signals received at two base station antennas and the average power received at the base station. The statistical averaging implied by the correlation is over instantiations of the clutter, often measured in practice by averaging the quantity of interest (e.g., power received) while translating the mobile antenna over several wavelengths.

The correlation of the fields (5) evaluated at base antenna locations $\mathbf{r}_1$ and $\mathbf{r}_2$ is expressed using (7), as shown in (9) at the bottom of the following page, where the field correlation in the plane $z' = 0$ is defined as $R_u = \langle U(\mathbf{r}'_1) U^*(\mathbf{r}'_2) \rangle$ and both base antennas are taken to be at the same height z. Changing the coordinates of the integration to mean and difference coordinates, $x'_m = (x' + x'')/2$, $y'_m = (y' + y'')/2$ and $x'_d = x' - x''$, $y'_d = y' - y''$, where the prime coordinates refer to the aperture of integration and similar definitions apply to the unprimed coordinates of the base station antenna, the expression for the field correlation becomes (10), shown at the bottom of the following page. Choosing a coordinate system with $y_m = 0$ (base array laterally centered), (10) becomes (11), shown at the bottom of the following page. The correlation $R_u(x'_m, y'_m, x'_d, y'_d)$ depends on the details of the arrangement and material properties of buildings, trees, and other scatterers. To represent the effect of multiple scattering from ob-

jects around the mobile, we assume the field correlation function to be separable into a product of average field intensity $I(x'_m, y'_m) = \langle |U(x'_m, y'_m)|^2 \rangle$ and a factor describing the fine structure of the field as a superposition of plane waves uniformly distributed over all solid angles

$$\begin{aligned} &R_u(x'_m, y'_m, x'_d, y'_d) \\ &\quad = I(x'_m, y'_m) \frac{1}{4\pi k^2} \int_{-\infty}^{\infty} \int_{-\infty}^{\infty} dk_x dk_y e^{ik_x x'_d + ik_y y'_d} \\ &\quad = I(x'_m, y'_m) \frac{\pi}{k^2} \delta(x'_d) \delta(y'_d). \end{aligned} \tag{12}$$

The field correlation function (12) in the street aperture is thus an incoherent spatially "white" field with spatially dependent intensity $I(x'_m, y'_m)$. Alternatively, the angular spectrum at the mobile may be constrained to real angles only, $(k_x^2 + k_y^2) \leq k^2$, thus excluding evanescent waves, and leading to the accepted behavior of the field near the mobile, with a spatial coherence scale on the order of half-wavelength. It is found that such modifications, while significant in characterizing the field near the mobile, do not produce substantial changes in the following development of received power and field correlation at the base. Substituting (12) into (11), one obtains

$$\begin{aligned} \langle U(\mathbf{r}_1) U^*(\mathbf{r}_2) \rangle &= \left\langle \left| \frac{\partial G_e}{\partial z'} \right|^2_{z'=0} \right\rangle \\ &\quad \times e^{ikx_d} \int_{-\infty}^{\infty} \int_{-\infty}^{\infty} dx'_m dy'_m \frac{\pi}{k^2} I(x'_m, y'_m) e^{-iky'_m y_d / x}. \end{aligned} \tag{13}$$

The average intensity of the field in the vicinity of the mobile is taken to be that of a spherical wave emitted from a mobile located at (x_0, y_0, z_0) within the street aperture of width A and zero otherwise

$$\begin{aligned} I(x'_m, y'_m) &= \frac{P_T}{4\pi \left((z_c - z_0)^2 + {y'_m}^2 + (x'_m - x_0)^2 \right)}, \ x_0 \in [0, A] \\ &= 0, \qquad\qquad\qquad\qquad\qquad\quad , \ x_0 \notin [0, A] \end{aligned} \tag{14}$$

where the mobile height z_0 and clutter height z_c are relative to ground. Substituting (14) into (13) and evaluating the integral over y'_m leads to

$$\begin{aligned} &\langle U(\mathbf{r}_1) U^*(\mathbf{r}_2) \rangle \\ &\quad = \left\langle \left| \frac{\partial G_e}{\partial z'} \right|^2_{z'=0} \right\rangle e^{ikx_d} (2\pi)^2 \mathrm{e}^{-|y_d| (k\sqrt{(z_c - z_0)^2 + (x_0 - A/2)^2}/x)} \\ &\qquad \times \int_0^A dx'_m \frac{P_T \pi}{(4\pi k)^2 \sqrt{(z_c - z_0)^2 + (x'_m - x_0)^2}} \\ &\quad \approx \left\langle \left| \frac{\partial G_e}{\partial z'} \right|^2_{z'=0} \right\rangle e^{ikx_d} \mathrm{e}^{-|y_d| (k\sqrt{(z_c - z_0)^2 + (x_0 - A/2)^2}/x)} \\ &\qquad \times \frac{P_T A \pi}{4k^2 \sqrt{(z_c - z_0)^2 + \left(x_0 - \frac{A}{2}\right)^2}}. \end{aligned} \tag{15}$$

The last approximation in (15) follows from replacing the slowly varying integrand by its value in the middle of the street by setting $x'_m = A/2$. The average power received by an

---

$$\begin{aligned} \langle U(\mathbf{r}_1) U^*(\mathbf{r}_2) \rangle &= \left\langle \left| \frac{\partial G_e}{\partial z'} \right|^2_{z'=0} \right\rangle e^{ik(x_1 - x_2)} \\ &\quad \times \int_{-\infty}^{\infty} \int_{-\infty}^{\infty} dx' dy' \int_{-\infty}^{\infty} \int_{-\infty}^{\infty} dx'' dy'' e^{ik(x' - x'')} e^{ik\left((y_1 - y')^2 + x'^2\right)/2x} e^{-ik\left((y_2 - y'')^2 + x''^2\right)/2x} R_u(\mathbf{r'}_1, \mathbf{r'}_2) \end{aligned} \tag{9}$$

$$\begin{aligned} \langle U(\mathbf{r}_1) U^*(\mathbf{r}_2) \rangle &= \left\langle \left| \frac{\partial G_e}{\partial z'} \right|^2_{z'=0} \right\rangle e^{ikx_d} \\ &\quad \times \int_{-\infty}^{\infty} \int_{-\infty}^{\infty} dx'_m dy'_m \int_{-\infty}^{\infty} \int_{-\infty}^{\infty} dx'_d dy'_d R_u(x'_m, y'_m, x'_d, y'_d) e^{-ikx'_d} e^{-ik\left(y_m y'_d + y'_m y_d + y_m y_d + y'_m y'_d\right)/x} e^{ikx'_m x'_d / x}. \end{aligned} \tag{10}$$

$$\begin{aligned} \langle U(\mathbf{r}_1) U^*(\mathbf{r}_2) \rangle &= \left\langle \left| \frac{\partial G_e}{\partial z'} \right|^2_{z'=0} \right\rangle e^{ikx_d} \\ &\quad \times \int_{-\infty}^{\infty} \int_{-\infty}^{\infty} dx'_m dy'_m \int_{-\infty}^{\infty} \int_{-\infty}^{\infty} dx'_d dy'_d R_u(x'_m, y'_m, x'_d, y'_d) e^{-ikx'_d} e^{-ik\left(y'_m y_d + y'_m y'_d\right)/x} e^{ikx'_m x'_d / x}. \end{aligned} \tag{11}$$

omnidirectional (unit-gain) antenna follows from evaluating (15) at $(x_d, y_d) = (0, 0)$

$$P_R = \lambda^2 \left\langle |U(\underline{r})|^2 \right\rangle = \lambda^2 \left\langle \left| \frac{\partial G_e}{\partial z'} \right|^2_{z'=0} \right\rangle \frac{P_T A \pi}{4k^2 \sqrt{(z_c - z_0)^2 + \left(x_0 - \frac{A}{2}\right)^2}}. \quad (16)$$

One may re-write (16) as

$$P_R = \lambda^2 \left\langle \left| \frac{\partial G_e}{\partial z'} \right|^2_{z'=0} \right\rangle L_{loc} P_T \quad (17)$$

where the local loss

$$L_{loc} = \frac{A\pi}{4k^2 \sqrt{(z_c - z_0)^2 + \left(x_0 - \frac{A}{2}\right)^2}} \quad (18)$$

is interpreted as the loss suffered on descent into the clutter in the vicinity of the mobile and $\langle |\partial G_e/\partial z'|^2_{z'=0} \rangle$ may be interpreted as the factor accounting for long range propagation over the generally varying terrain and clutter. For flat terrain with uniform height clutter, image theory may be used to determine $|\partial G_e/\partial z'|$ as in (4). Letting the height of the base above clutter be z, and recognizing that for most cases of interest, $z \ll x$, it is found that

$$\left\langle \left| \frac{\partial G_e}{\partial z'} \right|^2_{z'=0} \right\rangle \approx \frac{z^2}{\lambda^2 x^4}. \quad (19)$$

Using (18) and (19) in (17), the received power

$$P_R = \frac{z^2 A \pi}{4k^2 x^4 \sqrt{(z_c - z_0)^2 + \left(x_0 - \frac{A}{2}\right)^2}} P_T. \quad (20)$$

Path gain, defined as $P_G = 10\log_{10}(P_R/P_T)$ follows in closed form from (20). Path gain is naturally the negative of path loss: $P_G = -P_L$. As a reminder

z	is the base station height above clutter (m);
A	is the street width (m);
$k = 2\pi/\lambda$	is the wavenumber (m^{-1});
λ	is the wavelength (m);
x	is the range from transmitter to receiver (m);
z_c	is the height of clutter (e.g., buildings) above ground (m);
z_0	is the height of mobile above ground (m);
$x_0 \in [0, A]$	is the mobile location in the street, $x_0 = A/2$ for mobile in middle of street (m).

From (20), it may be observed that the received power P_R varies with frequency and distance to the base station in a way that is comparable to the empirical Hata model [2], as well as with the multiscreen diffraction model of Walfisch and Bertoni [6]. In particular, the received signal power decays with distance x as $1/x^4$. The virtue of the derivation here is that the field in the vicinity of the mobile is represented statistically in terms of the spectrum of plane waves, a generalization of the Jakes model [1]. Note that a single diffraction at the roof edge does not play an explicit role here, broadening the applicability of the formula to environments such as suburban streets lined with trees. Diffraction is however taken to be one of the scattering mechanisms leading to the diffuse structure of the field correlation in (12). Other contributions include diffracted and multiply-reflected components similar to those reported in ray-tracing studies for propagation around corners [8]. The widely reported small-scale fading around the mobile is in fact an indication that a single diffracted ray cannot be the only relevant propagation mechanism to access the mobile, and the field consists of many rays multiply scattered in the vicinity of the mobile and striking the roof edges at a wide range of angles. Roof edge diffraction may still be included by evaluating (11) using asymptotic end-point contributions from aperture edges, as was done in [9].

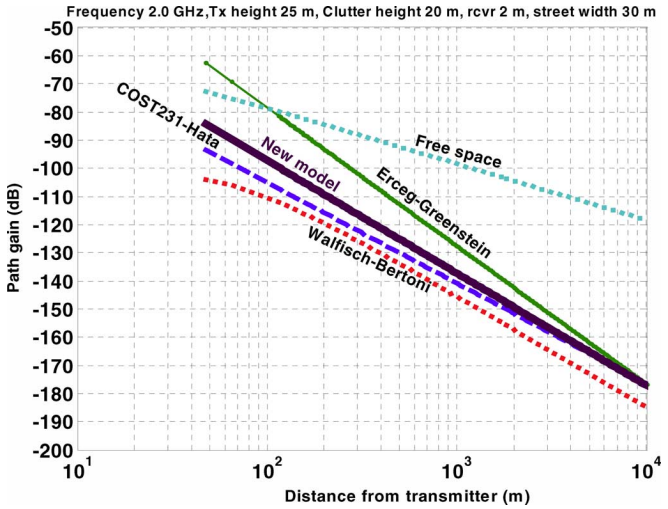

Fig. 2. Path gain over (urban) uniform height clutter predicted by several models as a function of range.

One consequence of such diffuse scattering is that the "keyhole" effect due to roof edge diffraction studied in [9] is not expected to occur for vertical array MIMO communications. The effective vertical angular spread observed at the base may still be narrow, possibly limiting capacity achievable with such arrays.

More generally, where there are significant terrain variations or varying clutter height, the Green's function derivative $\partial G_e/\partial z'$ needs to be re-derived to account for such cases.

The prediction for path gain P_G deduced from (20) is compared to other standard models, such as COST 231-Hata model [4], Walfisch–Bertoni multiscreen diffraction model [6] and the Erceg–Greenstein model [5] in Fig. 2. It may be observed that the new model appears to fall well within the range of predictions of standard models.

III. Spatial Correlation and Angular Spectra at the Base

Using (13) and (16), the received signal correlation at the two base antennas separated by y_d may be expressed as

$$\langle v(\mathbf{r}_1) v^*(\mathbf{r_2}) \rangle \approx P_R \, \mathrm{e}^{-|y_d|(k\sqrt{(z_c - z_0)^2 + (x_0 - A/2)^2}/x)} \quad (21)$$

where P_R is given by (20). The power angular spectrum of the field at the base antenna array may be found by Fourier trans-

forming the signal correlation (21) with respect to the base antenna separation y_d

$$P(k_y) = \int_{-\infty}^{\infty} dy_d \, \langle v(\mathbf{r}_1) v^*(\mathbf{r}_2) \rangle \, e^{ik_y y_d} \tag{22}$$

resulting in the Lorentzian power angular spectrum (PAS)

$$P(k_y) \approx P_R \frac{2a}{a^2 + k_y^2} \tag{23}$$

where $a = k\sqrt{(z_c - z_0)^2 + (x_0 - A/2)^2}/x$ and $k_y = k \sin\phi$. From (23) we see that for narrow angle spreads ($\sin\phi \approx \phi$) and mobile in the middle of the street ($x_0 = A/2$), the 3 dB point of the power angular spectrum

$$\phi_{3\ \mathrm{dB}} \approx \frac{a}{k} = \frac{(z_c - z_0)}{x}. \tag{24}$$

Measurements of power angular spectrum in the urban area of Aarhus have been reported in [13] for a high base station at base-mobile separations varying from 0.2 to 1.1 km. Rms angular spread for a high base station antenna is observed in [13, Fig. 5] to vary from 2° to 10° for the probability range (0.2,0.8). In [13] PAS was represented as a Laplacian function, $P(\phi) \propto \exp\left(-|\phi|\sqrt{2}/\sigma\right)$, with rms angular spread σ related to the 3 dB half-width $\phi_{3\ \mathrm{dB}}$ through $\phi_{3\ \mathrm{dB}} = \sigma \ln 2/\sqrt{2}$. For this form of PAS, the corresponding values of 3 dB half-width of the PAS are thus observed to vary from 1° to 5° for most of data in [13]. From (24) for 20 m high buildings ($z_c = 20$), the expected 3 dB point varies from 1° to 5° as range x varies from 1 km to 0.2 km. Furthermore, it has been reported in [19] that the Lorentzian forms an even better fit to measured angular spectra than the Laplacian based on the same data as [13]. In that work the Lorentzian has been found to follow from the statistical properties of low-resolution antennas independent of the actual spectrum. It follows from the analysis leading to (23) that the Lorentzian power angular spectrum is expected to arise from propagation modeling as well. We therefore conclude that both the predicted shape and width of the power angular spectrum are generally consistent with reported observations. We note that effects not considered here, such as scattering from clutter inhomogeneities, e.g., structures above the average clutter height, may increase the angle spread further, particularly for low base antennas. On the other hand, line of sight conditions between base and mobile may result in narrower effective angle spread. It should be mentioned that Blaunstein has reported close agreement between predicted and measured normalized angular and delay spectra in urban environment both for macrocellular [11] and for short-range microcellular cases [12]. The theoretical predictions applied in [11] and [12] treated building surfaces as rough and accounted for single and double scattering with shadowing and diffraction.

IV. Propagation for Mobile in Dense Vegetation

Tamir [21], [22] has analyzed propagation in the presence of vegetation by representing the vegetation as an effective medium described as a homogeneous dielectric slab for both terminals below clutter [21] and one terminal above clutter and one below [22]. The latter case is of interest in this paper as well. Considering frequencies below 200 MHz, the dominant propagation mechanism from the mobile immersed in clutter to a base above clutter was reported to be that of refraction at the canopy-air interface [22]. Tamir [22] has also pointed out that such effective medium representation is only valid for wavelengths larger than expected spacing between scatterers. Analysis of shorter wavelength propagation requires consideration of multiple scattering from trunks, branches and leaves.

In this paper, the vegetation is represented as a diffuse scattering and absorbing medium. Representing the tree canopy as a statistically homogeneous layer where the wave suffers diffuse scattering leads to the following picture: the field seen at the base is due to a "hot spot" on top of the trees, corresponding to the location right above the terminal. Propagation in free space over the tree canopy is described by (3). For low grazing angles relevant for base antenna heights z above canopy much smaller than range x, $z \ll x$, reflection from the canopy is given by $R_s \approx -1$, resulting in (4), as in the urban case with uniform height buildings. While tree canopy may not be expected to be perfectly flat, the approximation still holds for moderate canopy undulations provided that the rms surface roughness σ satisfies the Rayleigh criterion, $4\pi\sigma \sin\theta/\lambda \approx 4\pi\sigma z/\lambda x \ll 1$ [15], valid at large ranges x. Environments where the tree canopy is not continuous, as in the presence of sparsely growing trees or a forest clearing, are not treated here.

While propagation over the continuous tree canopy is represented, as before, by (4), somewhat different approach is required to describe propagation from the mobile through to the top of the vegetative layer to account for attenuation and scattering expected to occur near the mobile. Rich scattering expected at radio frequencies over 200 MHz leads to a spatially white process of the form (12). The field intensity $I(x'_m, y'_m)$ may be derived from the diffuse component of specific intensity [18]

$$I(x'_m, y'_m) = \left(\frac{\kappa_d}{4\pi r} + \frac{1}{4\pi r^2}\right) e^{-\kappa_d r} \tag{25}$$

where κ_d is the effective specific absorption in the diffuse medium, reported [20] to be on the order of 0.3 dB/m at 2 GHz, corresponding to 0.07 nepers/meter. The distance r from the mobile at $(0, 0, z_0)$ to a point (x'_m, y'_m, z_c) at the top of the vegetative clutter of height z_c is

$$r = \sqrt{(z_c - z_0)^2 + x'^2_m + y'^2_m} \approx (z_c - z_0) + \frac{x'^2_m + y'^2_m}{2(z_c - z_0)}. \tag{26}$$

The approximation in (26) is justified by recognizing that in heavily absorbing medium the main contribution to the field arriving at the base originates from scattered field right above the mobile. Substituting (25) into (13) and using (26), the field correlation at the base becomes

$$\langle U(\mathbf{r}_1) U^*(\mathbf{r}_2) \rangle = \left\langle \left| \frac{\partial G_e}{\partial z'} \right|^2_{z'=0} \right\rangle e^{ikx_d} \cdot \int_{-\infty}^{\infty} \int_{-\infty}^{\infty} dx'_m dy'_m \frac{\pi}{k^2} \left(\frac{\kappa_d}{4\pi r} + \frac{1}{4\pi r^2}\right) e^{-\kappa_d r} e^{-iky'_m y_d/x}. \tag{27}$$

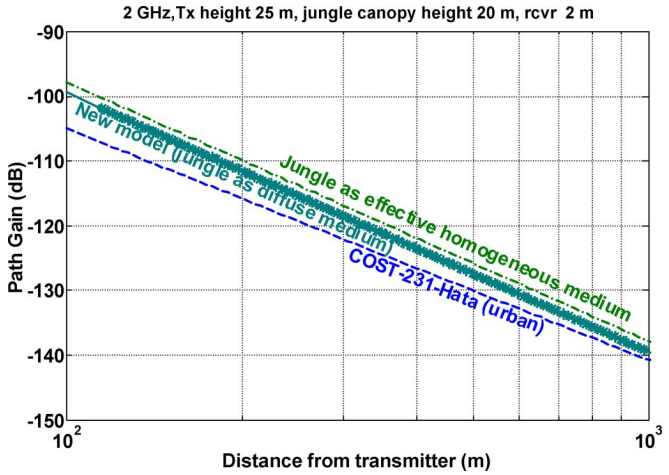

Fig. 3. Predicted path gain for diffuse medium jungle model (30) and for Tamir's model of jungle as effective (lossy dielectric) homogeneous medium.

For high loss (or tall vegetation), $1/\kappa_d \ll z_c - z_0$, and (27) becomes

$$\begin{aligned}
&\langle U(\mathbf{r}_1)U^*(\mathbf{r}_2)\rangle \\
&= \left\langle \left|\frac{\partial G_e}{\partial z'}\right|^2_{z'=0} \right\rangle e^{ikx_d}\frac{\pi}{k^2}e^{-\kappa_d(z_c-z_0)} \\
&\quad \int_{-\infty}^{\infty}\int_{-\infty}^{\infty} dx'_m dy'_m \left(\frac{\kappa_d}{4\pi\,(z_c-z_0)} + \frac{1}{4\pi(z_c-z_0)^2}\right) \\
&\quad \times e^{-\kappa_d((x'_m{}^2+y'_m{}^2)/2(z_c-z_0))}e^{-iky'_m y_d/x} \\
&\approx \left\langle \left|\frac{\partial G_e}{\partial z'}\right|^2_{z'=0} \right\rangle e^{ikx_d}e^{-\kappa_d(z_c-z_0)}\frac{\pi^2}{k^2} \\
&\quad \times \left(\frac{\kappa_d}{4\pi\,(z_c-z_0)} + \frac{1}{4\pi(z_c-z_0)^2}\right) \\
&\quad \times \frac{2\,(z_c-z_0)}{\kappa_d}e^{-k^2(z_c-z_0)y_d^2/2\kappa_d x^2}. \qquad (28)
\end{aligned}$$

Received power may be obtained from (28)

$$P_R = \lambda^2\left\langle \left|\frac{\partial G_e}{\partial z'}\right|^2_{z'=0} \right\rangle e^{-\kappa_d(z_c-z_0)}\frac{2\pi^2}{k^2}\left(\frac{1}{4\pi}+\frac{1}{4\pi(z_c-z_0)\,\kappa_d}\right)P_T. \qquad (29)$$

For flat terrain (19) may be used, resulting in

$$P_R = \frac{\pi z^2}{2k^2x^4}e^{-\kappa_d(z_c-z_0)}\left(1+\frac{1}{(z_c-z_0)\,\kappa_d}\right)P_T. \qquad (30)$$

The path gain $P_G = 10\log_{10}(P_R/P_T)$ obtained from (30) is plotted against range x in Fig. 3. Also plotted is the result derived by Bertoni [24], following Tamir [22], where the jungle has been treated as an effective (lossy dielectric) homogeneous medium and important effects are that of refraction at the canopy-air interface, as well as absorption loss within the effective dielectric medium representing the vegetation. Although the treatment of the vegetation as an effective medium includes only the coherent wave, and is thus valid only for low frequencies (below 25 MHz), the predicted path gain levels are very close when the effective medium model is evaluated at the same high frequency (2 GHz) as the diffuse medium model (30). It should be noted that reported observation of half-wavelength scale spatial variation in vegetation [25], attributed to multiple scattering, is consistent with the diffuse model employed here. Treating the vegetation as homogeneous medium results in a single refracted signal with nearly planar wave front, and no small-scale spatial variation.

For flat terrain, using (28) and (30), the received signal correlation at two base antennas separated by y_d may be expressed as

$$\langle v(\mathbf{r}_1)v^*(\mathbf{r}_2)\rangle \approx P_R e^{-k^2(z_c-z_0)y_d^2/2\kappa_d x^2} \qquad (31)$$

where P_R is given by (30). The power angular spectrum is found to have a Gaussian form as follows from the Fourier transform (22) of (31) with respect to antenna separation y_d

$$P(k_y) \approx P_R b\sqrt{2\pi}e^{-b^2k_y^2/2} \qquad (32)$$

where $b = (x/k)\sqrt{\kappa_d/(z_c-z_0)}$ and $k_y = k\sin\phi$. For $bk \gg 1$, the rms angle spread σ_{AS} follows from (32) as $\sigma_{AS} = 1/bk$. At 2 GHz, range of $x = 1000$ m, canopy height $z_c = 10$ m, mobile height $z_0 = 2$ m, specific absorption loss $\kappa_D = 0.07$ nepers/meter, the rms angle spread at the base is computed to be 0.6°.

V. Conclusion

Propagation of radio signals from a base above clutter, such as buildings and trees to a mobile immersed in clutter, is treated theoretically by accounting for random diffuse scattering at the mobile. Closed form expressions are derived for path gain as well as for angular spectrum at the base. The resulting predictions are in close agreement with widely accepted models and empirical results. The angular spectrum at the base in urban environment is found to be Lorentzian of width close to that reported in measurements in Aarhus. Vegetation is represented as statistically homogeneous diffuse scattering medium, resulting in a Gaussian-shaped angular spectrum at the base. Small-scale fading and distance-dependent loss are treated in a unified way, as opposed to the heuristic methodologies, which formulate them as separate factors.

References

[1] W. C. Jakes, Ed., Microwave Mobile Communications. New York, Wiley, 1974.
[2] M. Hata, "Empirical formula for propagation loss in land mobile radio services," *IEEE Trans. Veh. Technol.*, vol. 29, no. 3, pp. 317–325, Aug. 1980.
[3] Y. Okumura, E. Ohmori, T. Kawano, and K. Fukuda, "Field strength and its variability in VHF and UHF land-mobile radio service," *Rev. Elect. Com. Lab.*, vol. 16, pp. 825–873, 1968.
[4] "Digital Mobile Radio Towards Future Generation Systems, Final Report, " Tech. Rep. COST Action 231, 1999, European Communities, EUR 18957.
[5] V. Erceg, L. J. Greenstein, S. Y. Tjandra, S. R. Parkoff, A. Gupta, B. Kulic, A. A. Julius, and R. Bianchi, "An empirically based path loss model for wireless channels in suburban environments," *IEEE J. Sel. Areas Commun.*, vol. 17, pp. 1205–1211, Jul. 1999.
[6] J. Walfisch and H. L. Bertoni, "A theoretical model of UHF propagation in urban environments," *IEEE Trans. Antennas Propag.*, vol. 36, no. 12, pp. 1788–1796, Dec. 1988.

[7] J. H. Whitteker, "Physical optics and field-strength predictions for wireless systems," *IEEE J. Select. Areas Commun.*, vol. 20, pp. 515–522, Apr. 2002.
[8] V. Erceg, A. J. Rustako, Jr, and R. S. Roman, "Diffraction around corners and its effects on the microcell coverage area in urban and suburban environments at 900 MHz, 2 GHz, and 4 GHz," *IEEE Trans. Veh. Technol.*, vol. 43, no. 3, pp. 762–766, Aug. 1994.
[9] D. Chizhik, G. J. Foschini, M. J. Gans, and R. A. Valenzuela, "Keyholes, correlations, and capacities of multielement transmit and receive antennas," *IEEE Trans. Wireless Commun.*, vol. 1, no. 2, pp. 361–368, Apr. 2002.
[10] N. Blaunstein, D. Katz, D. Censor, A. Freedman, I. Matityahu, and I. Gur-Arie, "Prediction of loss characteristics in built-up areas with various buildings' overlay profiles," *IEEE Antennas Propag. Mag.*, vol. 43, no. 6, pp. 181–191, Dec. 2001.
[11] N. Blaunstein, "Distribution of angle-of-arrival and delay from array of buildings placed on rough terrain for various elevations of base station antenna," *J. Commun. Networks*, vol. 2, no. 4, pp. 305–316, Dec. 2000.
[12] N. Blaunstein, M. Toeltsch, J. Laurila, E. Bonek, D. Katz, P. Vainikainen, N. Tsouri, K. Kalliola, and H. Laitinen, "Signal power distribution in the azimuth, elevation and time delay domains in urban environments for various elevations of base station antenna," *IEEE Trans. Antennas Propag.*, vol. 54, no. 10, pp. 2902–2916, Oct. 2006.
[13] T.-S. Chu and L. J. Greenstein, "A semiempirical representation of antenna diversity gain at cellular and PCS base stations," *IEEE Trans. Commun.*, vol. 45, no. 6, pp. 644–646, Jun. 1997.
[14] C. A. Balanis, *Advanced Engineering Electromagnetics*. New York: Wiley, 1989.
[15] P. Beckmann and A. Spezzichino, *The Scattering of Electromagnetic Waves from Rough Surfaces*. Boston, MA: Artech House, 1987.
[16] A. J. Rustako Jr., N. Amitay, G. J. Owens, and R. S. Roman, "Radio propagation at microwave frequencies for line-of-sight microcellular mobile and personal communications," *IEEE Trans. Veh. Technol.*, vol. 40, no. 1, pp. 203–210, Feb. 1991.
[17] A. Kuchar, J.-P. Rossi, and E. Bonek, "Directional macro-cell channel characterization from urban measurements," *IEEE Trans. Antennas Propag.*, vol. 48, no. 2, pp. 139–146, Feb. 2000.
[18] K. I. Pedersen, P. E. Mogensen, and B. H. Fleury, "A stochastic model of the temporal and azimuthal dispersion seen at the base station in outdoor propagation environments," *IEEE Trans. Veh. Technol.*, vol. 49, no. 2, pp. 437–447, Mar. 2000.
[19] A. Ishimaru, *Wave Propagation and Scattering in Random Media*. Piscataway, NJ: IEEE Press, 1997.
[20] J. B. Andersen and K. I. Pedersen, "Angle-of-arrival statistics for low resolution antennas," *IEEE Trans. Antennas Propag.*, vol. 50, no. 3, pp. 391–395, Mar. 2002.
[21] T. Tamir, "On radio-wave propagation in forest environments," *IEEE Trans. Antennas Propag.*, vol. 15, pp. 806–817, Nov. 1967.
[22] T. Tamir, "Radio wave propagation along mixed paths in forest environments," *IEEE Trans. Antennas Propag.*, vol. 25, pp. 471–477, Jul. 1977.
[23] G. S. Brown and W. J. Curry, "A theory and model for wave propagation through foliage," *Radio Sci.*, vol. 17, no. 5, pp. 1027–1036.
[24] H. L. Bertoni, *Radio Propagation for Modern Wireless Systems*. Englewood Cliffs, NJ: Prentice Hall, 2000.
[25] "Tropical Propagation Research", Final Rep. Jansky and Bailey Eng. Dept., 1967, vol. 1, Atlantic Research Corp., (NTIS AD660318).

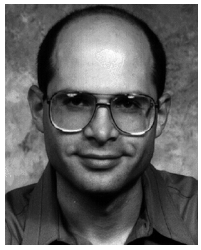

Dmitry Chizhik received the Ph.D. degree in electrophysics from the Polytechnic University, Brooklyn, NY, in 1991. His thesis work was in ultrasonics and non-destructive evaluation.

Previously, he was with the Naval Undersea Warfare Center, New London, CT, where he did research in scattering from ocean floor, geoacoustic modeling and shallow water acoustic propagation. Since 1996, he has been a member of Technical Staff in the Wireless Research Laboratory, Bell Labs, Alcatel-Lucent , Holmdel, NJ, working on radio propagation modeling and measurements, using deterministic and statistical techniques. His recent work has been in measurement, modeling and channel estimation of MIMO channels. The results are used both for determination of channel-imposed bounds on channel capacity, system performance, as well as for optimal antenna array design. His research interests are in acoustic and electromagnetic wave propagation, signal processing, and communications.

Jonathan Ling received the B.Sc. degree in electrical engineering from Rutgers University, Piscataway, NJ, in 1992, and the M.Sc. degree in computer science and the Ph.D. degree in electrical engineering both from Stevens Institute, Hoboken, NJ, in 1999 and 2008, respectively.

He joined the Wireless Communications Research Department, Bell Laboratories, Lucent Technologies, Holmdel, NJ, in 1994. He has conducted MIMO radio propagation measurements and modeling, and developed the WiSE ray-tracing tool. His research interests are channel modeling and signal processing.